Low-Density Self-Assembled Monolayers on Gold Derived from Chelating 2-Monoalkylpropane-1,3-dithiols

Young-Seok Shon,† Ramon Colorado, Jr.,† Christopher T. Williams,‡ Colin D. Bain,‡ and T. Randall Lee*,†

Department of Chemistry, University of Houston, Houston, Texas 77204-5641, and Physical and Theoretical Chemistry Laboratory, University of Oxford, Oxford OX1 3QZ, U.K.

Received December 8, 1998. In Final Form: August 12, 1999

Low-density self-assembled monolayers (SAMs) on gold were generated by the adsorption of a series of specifically designed 2-monoalkylpropane-1,3-dithiol derivatives, $CH_3(CH_2)_nCH[CH_2SH]_2$, where $n =$ 11, 13, 14. The monolayers were characterized by optical ellipsometry, X-ray photoelectron spectroscopy, contact angle goniometry, polarization modulation infrared reflection absorption spectroscopy, and sum-frequency generation. Comparison of these data to those collected on SAMs generated from normal alkanethiols, $CH_3(CH_2)_{n+2}SH$, and 2,2-dialkylpropane-1,3-dithiol derivatives, $[CH_3(CH_2)_n]_2C[CH_2SH]_2$, of similar chain length suggests that the new "monoalkanedithiol" SAMs are the least crystalline, exposing both methyl and methylene groups at the interface due to the low density of alkyl chains. Further comparison of these low-density SAMs to those obtained on branched and linear polyethylene films suggests that the exposure of interfacial methylene groups is greater for the polymer films.

Introduction

The ability to manipulate the interfacial properties of organic surfaces represents a useful tool in technological applications involving adhesion, tribology, and corrosion.[1,2] To examine these phenomena in detail, organic monolayer films have been used to provide the level of structural control required for meaningful analysis and interpretation.[3] Perhaps the most popular system currently used to explore the properties of organic surfaces is that of self-assembled monolayers (SAMs) generated from well-characterized organic adsorbates.[4−8] Commonly encountered organic surfaces such as those found in polymeric materials, however, differ from the highly ordered and densely packed model interfaces generated from this approach.[9] Consequently, SAM research has evolved a number of strategies aimed at generating complex but still well-defined organic interfaces. One approach involves the coadsorption of two or more organic compounds having different functional groups and/or different chain lengths (e.g., mixtures of ω-functionalized alkanethiols adsorbed onto gold).[10−14] These types of studies, however, are often hampered by the fact that the coadsorption process is governed by several factors, such as the differing solubilities of mixed adsorbates as well as kinetic and/or thermodynamic preferential adsorption of one of the species. As a consequence, coadsorption often leads to inhomogeneous mixing[15] and/or domain formation (known as "islanding").[12,16] A second approach designed to yield complex interfaces involves the use of tethered difunctional adsorbates (e.g., unsymmetrical alkyl disulfides adsorbed onto gold); this approach too, however, suffers from potential islanding effects, as it is known that the disulfides dissociate upon adsorption to the surface of gold.[17] While the adsorption of unsymmetrical sulfides onto gold can be used to circumvent the islanding issue, the poor stability of the resultant SAMs has limited their utility.[18,19]

One of the goals of our research in organic thin films is the preparation of well-defined model interfaces in which the alkyl chains are loosely packed. These model interfaces should closely resemble polymer surfaces, where the alkyl chains are typically highly disordered with many degrees of freedom.[20] Well-defined loosely packed interfaces can thus provide a useful system for examining the microscopic factors that give rise to macroscopic surface properties ranging from wettability and permeability to adhesion and friction.

In this report, we describe a new class of well-defined organic thin films generated by the adsorption of chelating 2-monoalkylpropane-1,3-dithiols (**1**−**3**, Figure 1) onto the surface of gold. Recently, we showed that densely packed and highly ordered SAMs could be prepared similarly from 2,2-dialkylpropane-1,3-dithiols (**4**−**6**, "spiroalkanedithiols").[21] In the present work, we reasoned that SAMs

† University of Houston.

‡ University of Oxford.

(1) Ulman, A. *An Introduction to Ultrathin Organic Films*; Academic: Boston, 1991.
(2) Whitesides, G. M. *Sci. Am.* **1995**, *9*, 146.
(3) Ulman, A. *Chem. Rev.* **1996**, *96*, 1533.
(4) Porter, M. D.; Allara, D. L.; Chidsey, C. E. D. *J. Am. Chem. Soc.* **1987**, *109*, 3559.
(5) Bain, C. D.; Whitesides, G. M. *J. Am. Chem. Soc.* **1988**, *110*, 5897.
(6) Bain, C. D.; Troughton, E. B.; Tao, Y.-T.; Evall, J.; Whitesides, G. M.; Nuzzo, R. G. *J. Am. Chem. Soc.* **1989**, *111*, 321.
(7) Whitesides, G. M.; Laibinis, P. E. *Langmuir* **1990**, *6*, 87.
(8) Lee, T. R.; Carey, R. I.; Biebuyck, H. A.; Whitesides, G. M. *Langmuir* **1994**, *10*, 741.
(9) Bain, C. D.; Whitesides, G. M. *Angew. Chem., Int. Ed. Engl.* **1989**, *28*, 506.
(10) Bain, C. D.; Whitesides, G. M. *J. Am. Chem. Soc.* **1989**, *111*, 7164 and references therein.
(11) Folkers, J. P.; Laibinis, P. E.; Whitesides, G. M. *Langmuir* **1992**, *8*, 1330.
(12) Folkers, J. P.; Laibinis, P. E.; Whitesides, G. M.; Deutch, J. *J. Phys. Chem.* **1994**, *98*, 563.
(13) Jin, Z. H.; Vezenov, D. V.; Lee, Y. W.; Zull, J. E.; Sukenik, C. N.; Savineil, R. F. *Langmuir* **1994**, *10*, 2662.
(14) Creager, S. E.; Clarke, J. *Langmuir* **1994**, *10*, 3675.
(15) Stranick, S. J.; Parikh, A. N.; Tao, Y.-T.; Allara, D. L.; Weiss, P. S. *J. Phys. Chem.* **1994**, *98*, 7636.
(16) Tamada, K.; Hara, M.; Sasabe, H.; Knoll, W. *Langmuir* **1997**, *13*, 1558.
(17) Biebuyck, H. A.; Whitesides, G. M. *Langmuir* **1993**, *9*, 1766.
(18) Troughton, E. B.; Bain, C. D.; Whitesides, G. M. *Langmuir* **1988**, *4*, 365.
(19) Zhang, M.; Anderson, M. *Langmuir* **1994**, *10*, 2807.
(20) Sun, F.; Castner, D. G.; Grainger, D. W. *Langmuir* **1993**, *9*, 3200.
(21) Shon, Y.-S.; Lee, T. R. *Langmuir* **1999**, *15*, 1136.

10.1021/la981698l CCC: $19.00
Published on Web 10/21/1999

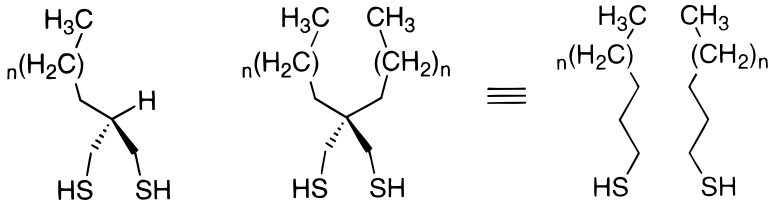

n = 10	**(C14)**	**1**	**4**	**7**
n = 12	**(C16)**	**2**	**5**	**8**
n = 13	**(C17)**	**3**	**6**	**9**
		m	**d**	**n**

Figure 1. Structures of the spiroalkanedithiols and normal alkanethiols used for generating SAMs on gold.

Scheme 1

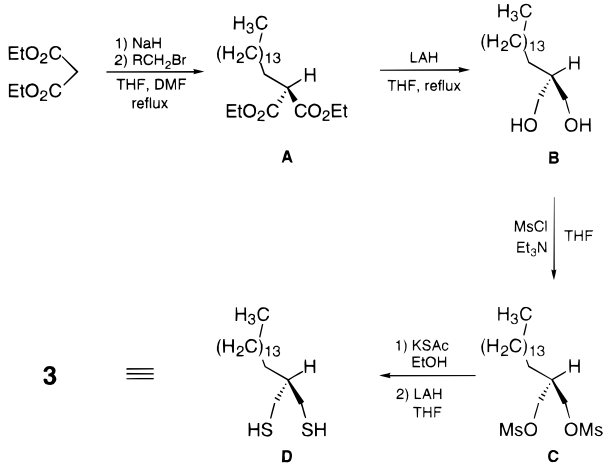

generated from monoalkyl versions of these dithiols would have a lower density of alkyl chains than those generated from the parent system (or from normal alkanethiols, **7**−**9**). We further anticipated that the "monoalkanedithiols" would provide an array of alkyl chains with regular spacing due to the uniform anchoring of the chelating dithiol moieties to the surface of gold. Additionally, we felt that the use of the monoalkanedithiols would exclude the possibility of inhomogeneous mixing and/or islanding.

Experimental Section

Synthesis of 2-Monoalkylpropane-1,3-dithiols. The majority of the materials for the synthesis of the adsorbates have been described in detail in a previous report.[21] The strategy used to synthesize the 2-monoalkylpropane-1,3-dithiols is shown in Scheme 1, using compound **3** as a representative target. We provide below a general procedure for each step of the synthesis. Complete analytical data are provided for all 2-monoalkylpropane-1,3-dithiol final products.

*Diethyl 2-pentadecylmalonate (**A**).* A solution of NaH (6.00 g; 150 mmol) in THF (250 mL) and DMF (75 mL) was prepared at 0 °C under argon. To this solution, diethyl malonate (24.9 g; 150 mmol) was added slowly. The mixture was stirred at room temperature for 15 min, and then bromopentadecane (14.6 g; 50.0 mmol) was added, and the mixture heated under reflux for 2 h. The reaction mixture was concentrated under vacuum, and the resultant oil was suspended in 100 mL of water. The mixture was extracted first with pentane (2 × 100 mL) and then with a 1:1 mixture of pentane/diethyl ether (1 × 100 mL). The organic layers were washed with H_2O (3 × 50 mL), dried over $MgSO_4$, and evaporated to dryness. The crude product was purified by vacuum distillation to afford diethyl 2-pentadecylmalonate in 93% yield. ^{1}H NMR (300 MHz, $CDCl_3$): δ 4.19 (q, J = 7.3 Hz, 4 H, OCH_2), 3.31 (t, J = 8.3 Hz, 1 H, C(O)CH), 1.87 (m, 2 H, CH_2-CH), 1.36−1.20 (m, 32 H), 0.88 (t, J = 7.7 Hz, 3 H, CH_3). ^{13}C NMR (75 MHz, $CDCl_3$): δ 169.6, 61.2, 31.9, 29.7, 29.6, 29.34, 29.31, 29.2, 28.8, 27.3, 22.7, 14.1.

*2-Pentadecylpropane-1,3-diol (**B**).* Lithium aluminum hydride (LAH; 1.31 g; 34.6 mmol) was added to a solution of diester **A** (3.50 g; 8.66 mmol) in THF at room temperature, and the reaction mixture was heated under reflux for 2 h. The reaction was quenched by the addition of 150 mL of a 1 M HCl solution and stirred for 30 min. The aqueous layer was extracted with diethyl ether (3 × 75 mL). The combined organic layers were washed with dilute HCl solution (2 × 75 mL) and brine (1 × 75 mL), and then dried over $MgSO_4$. Removal of the solvents under vacuum afforded crude 2-pentadecylpropane-1,3-diol in 95% yield. ^{1}H NMR (300 MHz, $CDCl_3$): δ 3.82 (d of d, J_{vic} = 4.0 Hz, J_{gem} = 12.0 Hz, 2 H, CH_2OH), 3.66 (d of d, J_{vic} = 8.7 Hz, J_{gem} = 12.0 Hz, 2 H, CH_2OH), 1.78 (m, 1 H, CH), 1.38−1.20 (m, 28 H), 0.88 (t, J = 7.7 Hz, 3 H, CH_3). ^{13}C NMR (75 MHz, $CDCl_3$): δ 66.8, 31.9, 29.7, 29.6, 29.4, 29.2, 28.8, 27.2, 22.7, 14.1.

*2-Pentadecylpropane-1,3-dimesylate (**C**).* A solution of diol **B** (2.24 g; 7.83 mmol) and triethylamine (1.98 g; 19.6 mmol) in THF was prepared. To the stirred mixture, 2.24 g (19.6 mmol) of methanesulfonyl chloride were added dropwise over 5 min. After the addition was complete, stirring was continued for 2 h. Ice-cold water (100 mL) was poured into the reaction mixture to destroy any excess methanesulfonyl chloride. The aqueous layer was separated from the organic layer and extracted with dichloromethane (3 × 50 mL). The organic phases were combined and washed with dilute HCl (1 × 50 mL), H_2O (1 × 50 mL), $NaHCO_3$ solution (2 × 50 mL), and H_2O (1 × 50 mL). The organic layer was dried over $MgSO_4$, and the solvent was removed by rotary evaporation to give the crude dimesylate in 97% yield. ^{1}H NMR (300 MHz, $CDCl_3$): δ 4.29 (d of d, J_{vic} = 4.7 Hz, J_{gem} = 11.3 Hz, 2 H, CH_2OMs), 4.19 (d of d, J_{vic} = 7.0 Hz, J_{gem} = 11.3 Hz, 2 H, CH_2OMs), 3.05 (s, 6 H, OMs), 2.16 (m, 1 H, CH), 1.38−1.20 (m, 28 H), 0.88 (t, J = 7.7 Hz, 3 H, CH_3). ^{13}C NMR (75 MHz, $CDCl_3$): δ 68.2, 37.3, 31.9, 29.7, 29.6, 29.5, 29.4, 29.3, 27.0, 22.7, 14.1.

*2-Pentadecylpropane-1,3-dithiol (**D, 3**).* Potassium thioacetate (1.94 g; 17.0 mmol) and dimesylate **C** (3.00 g; 6.79 mmol) were placed in 100 mL of EtOH under argon and heated to 70 °C for 6 h. Water (100 mL) was added, and the mixture was extracted with diethyl ether (3 × 100 mL). The organic phases were washed with H_2O (3 × 100 mL) and then dried over $MgSO_4$. The crude products were dissolved in THF, and LAH (1.03 g; 27.2 mmol) was added at room temperature. The mixture was heated under reflux for 2 h and then quenched under argon with ethanol (20 mL; previously degassed by bubbling with argon). After being stirred for 10 min, the mixture was acidified to ca. pH 1 by the careful addition of 1 M HCl. The aqueous layer was extracted with diethyl ether (3 × 50 mL). The combined organic layers were washed with dilute HCl solution (2 × 50 mL) and brine (1 × 50 mL), and then dried over $MgSO_4$. The solvents were evaporated under vacuum, and the crude products were purified by column chromatography on silica gel using hexane as the eluant to give 2-pentadecylpropane-1,3-dithiol in 88% yield. ^{1}H NMR (300 MHz, $CDCl_3$): δ 2.76−2.58 (m, 4 H, CH_2SH), 1.67 (m, 1 H, CH), 1.38−1.22 (m, 28 H), 1.19 (t, J = 9.3 Hz, 2 H, SH), 0.88 (t, J = 7.7 Hz, 3 H, CH_3). ^{13}C NMR (75 MHz, $CDCl_3$): δ 42.6, 31.9,

31.4, 29.7, 29.64, 29.60, 29.5, 29.4, 26.9, 26.7, 22.7, 14.1. Anal. Calcd for $C_{17}H_{36}S_2$: C, 67.85; H, 12.02. Found: C, 67.59; H, 11.62.

*2-Dodecylpropane-1,3-dithiol (**1**).* ^{1}H NMR (300 MHz, $CDCl_3$): δ 2.76−2.58 (m, 4 H, CH_2SH), 1.67 (m, 1 H, C*H*), 1.38−1.20 (m, 22 H), 1.20 (t, $J = 9.3$ Hz, 2 H, S*H*), 0.88 (t, $J = 7.7$ Hz, 3 H, CH_3). ^{13}C NMR (75 MHz, $CDCl_3$): δ 42.6, 31.9, 31.4, 29.7, 29.6, 29.5, 29.4, 26.9, 26.7, 22.7, 14.1. HRMS Calcd for $C_{15}H_{32}S_2$: 276.1945. Found: 276.1938(3).

*2-Tetradecylpropane-1,3-dithiol (**2**).* ^{1}H NMR (300 MHz, $CDCl_3$): δ 2.76−2.58 (m, 4 H, CH_2SH), 1.67 (m, 1 H, C*H*), 1.38−1.20 (m, 26 H), 1.20 (t, $J = 9.3$ Hz, 2 H, S*H*), 0.88 (t, $J = 7.7$ Hz, 3 H, CH_3). ^{13}C NMR (75 MHz, $CDCl_3$): δ 42.6, 31.9, 31.4, 29.67, 29.65, 29.60, 29.55, 29.4, 26.9, 26.8, 22.7, 14.1. Anal. Calcd for $C_{17}H_{36}S_2$: C, 67.04, H, 11.91. Found: C, 67.48, H, 11.67.

Preparation of SAMs. The majority of the materials and methods used to prepare gold-coated Si wafers has been described in detail in a previous report.[21] Adsorptions were carried out in glass weighing bottles that had been precleaned by soaking for 1 h in "piranha" solution (7.5:2.5, H_2SO_4/H_2O_2); *caution: "piranha" solution reacts violently with organic materials, and should be handled carefully.* The bottles were rinsed with deionized water and absolute ethanol, and dried overnight at ≥100 °C. The slides were washed with absolute ethanol and dried under a flow of ultrapure nitrogen before immersion in solution. The slides were immersed in solutions (ca. 1 mM) of the chelating alkanedithiols (**1**−**6** in isooctane) and normal alkanethiols (**7**−**9** in ethanol). The monolayers were allowed to equilibrate for a period of 48 h. The resultant SAMs were exhaustively rinsed with toluene and ethanol and were dried under a flow of ultrapure nitrogen before analysis.

Characterization of SAMs. The instruments and methods used to collect the ellipsometry, contact angle goniometry, and polarization modulation infrared reflection absorption spectroscopy (PM-IRRAS) data have been described in detail in a previous report.[21] The SAMs examined here were additionally characterized by X-ray photoelectron spectroscopy (XPS) and sum-frequency generation (SFG); the experimental details of these latter characterizations are described in the following two paragraphs.

A PHI 5700 X-ray photoelectron spectrometer equipped with a monochromatic Al Kα X-ray source ($h\nu = 1486.7$ eV) incident at 90° relative to axis of a hemispherical energy analyzer was used to obtain X-ray photoelectron spectra of freshly prepared samples. The spectrometer was configured to operate at high resolution with a pass energy of 23.5 eV, a photoelectron takeoff angle of 45° from the surface, and an analyzer spot diameter of 1.1 mm. Spectra were collected at room temperature and a base pressure of 2×10^{-9} Torr for the following elements: $C_{(1s)}$ (8 scans over 1.67 min), $S_{(2p)}$ (40 scans over 6.67 min), and $Au_{(4f)}$ (4 scans over 0.67 min). Standard curve-fitting software (Shirley background subtraction; Gaussian−Lorentzian profiles) was used to determine the peak intensities. All peaks were fit with respect to spin−orbit splitting. A 100% Gaussian curve was used for the $C_{(1s)}$ peaks. Two 80% Gaussian curves in a 1:2 ratio of areas split at 1.18 eV were used for the $S_{(2p)}$ peaks, and two 65% Gaussian curves in a 3:4 ratio of areas split by 3.67 eV were used for the $Au_{(4f)}$ peaks.

The sum-frequency spectrometer has been described in detail elsewhere.[22] The green and infrared laser beams were incident on the gold surface in a counterpropagating geometry with angles of incidence of 50° and 60°, respectively. The respective energies of the IR and green pulses were ca. 0.5 and 2.7 mJ. The area of overlap of the two beams on the gold surface was ca. 3 mm^2. The detected sum-frequency signal was normalized by the intensity of the infrared laser. SFG spectra were acquired for compounds **m-C16** (**2**), **d-C16** (**5**), and **n-C16** (**8**) with both ppp and ssp polarizations (where the letters refer to the polarizations of the sum-frequency, green, and infrared fields in order). The acquisition times were 50 min for both ppp and ssp polarized spectra. The algorithm used to fit the SF spectra has been described elsewhere.[23] Each peak was characterized by four parameters: a line strength, S, a resonant frequency, ω, a Lorentzian line width, Γ (to represent homogeneous broadening), and a Gaussian line width, σ (to represent inhomogeneous broadening). To fit SF spectra of hydrocarbon chains, it is necessary to include most or all of the vibrations in the C−H stretching region. The assignment of the observed modes is given below;[24,25] the wavenumbers in parentheses are those observed in SAMs derived from **m-C16**. The symmetric methyl stretch ($\upsilon_s^{CH_3}$; r^+) is split by a Fermi resonance into two components (2878 and 2938 cm^{-1}), the antisymmetric methyl stretch ($\upsilon_a^{CH_3}$; r^-) as an in-plane component, r_a^- (2963 cm^{-1}), and an out-of-plane component, r_b^- (not observed in SAMs derived from **m-C16**, but typically around 2954 cm^{-1}). The methylene stretch is also split into symmetric ($\upsilon_s^{CH_2}$; d^+, 2853 cm^{-1}) and antisymmetric ($\upsilon_a^{CH_2}$; d^-, 2927 cm^{-1}) modes. The low-frequency shoulder (2868 cm^{-1}) on the r^+ mode is assigned to the $d^+{}_\omega$ mode.[26] The broad Fermi resonance of the d^+ mode (2890−2930 cm^{-1} in IR and Raman spectra[24]) was arbitrarily fitted with two peaks centered near 2897 and 2912 cm^{-1}. In addition, the nonresonant background from the gold was assigned a strength and phase. A number of constraints were applied to the fits. First, ω, σ, and Γ were required to have identical values in the ppp- and ssp-polarized spectra of the same monolayer. Second, the phase of the nonresonant background was constrained to the same value for all spectra with the same polarization. (The strength of the nonresonant background was not constrained in this fashion as it varied by less than 3%.) Finally, the overall line width ($\sigma + \Gamma$) was not permitted to vary by more than 0.5 cm^{-1} for the same vibration in different monolayers. With these constraints, it was possible to obtain good quality simultaneous fits to the six spectra, with the exception of the extreme high and low wavenumber regions of the ssp-polarized spectra.

Table 1. Ellipsometric Thicknesses (Å) of SAMs[a]

compound	C14	C16	C17
1−**3**	12.6	14.3	15.9
4−**6**	15.0	17.7	18.9
7−**9**	16.5	18.9	19.6

[a] We report average values of at least nine independent measurements. Measured values were always within ±2 Å of those reported.

Results

To compare SAMs generated from the monoalkanedithiols and spiroalkanedithiols to those generated from normal alkanethiols, we consider all adsorbates as "C_{n+2}" to reflect the overall number of carbon atoms in the primary chain (i.e., the number of carbon atoms along a given chain from the sulfhydryl group to the terminal methyl group as illustrated in Figure 1). Therefore, SAMs derived from $CH_3(CH_2)_{11}CH[CH_2SH]_2$, for example, would most readily correspond to a monolayer derived from $CH_3(CH_2)_{13}SH$ or a half-depleted monolayer derived from $[CH_3(CH_2)_{11}]_2C[CH_2SH]_2$.

Spectral ellipsometry provides a rough estimate of the degree of coverage of SAMs.[1] The data in Table 1 show that the ellipsometric thicknesses of the SAMs generated from the 2-monoalkylpropane-1,3-dithiols (**1**−**3**) are approximately 3 Å lower than those generated from the corresponding 2,2-dialkylpropane-1,3-dithiols (**4**−**6**) and approximately 4 Å lower than those generated from the corresponding normal alkanethiols (**7**−**9**). In these analyses, we assumed a refractive index of 1.45 for all films. The results suggest two important features regarding the SAMs generated from 2-monoalkylpropane-1,3-dithiols: (1) the new adsorbates generate monolayer rather than

(22) Bain, C. D. *J. Chem. Soc., Faraday Trans.* **1995**, *91*, 1281.
(23) Bain, C. D.; Davies, P. B.; Ong, T. H.; Ward, R. N.; Brown, M. A. *Langmuir* **1991**, *7*, 1563.
(24) Snyder, R. G.; Hsu, S. L.; Krimm, S. *Spectrochim. Acta* **1978**, *45A*, 395. MacPhail, R. A.; Strauss, H. L.; Snyder, R. G.; Elliger, C. A. *J. Phys. Chem.* **1994**, *88*, 334.
(25) Ward, R. N.; Duffy, D. C.; Davies, P. B.; Bain, C. D. *J. Phys. Chem.* **1994**, *98*, 8536.
(26) Goates, S. R.; Schofield, D. A.; Bain, C. D. *Langmuir* **1999**, *15*, 1400. Casson, B. D.; Bain, C. D. *J. Phys. Chem. B* **1999**, *103*, 4678.

Table 2. XPS Binding Energies (BEs) and Integrated Peak Areas of SAMs[a]

compound	$C_{(1s)}$ (eV)	$S_{(2p)}$ (eV)	$Au_{(4f)}$	$C_{(1s)}$
n-C16 (**8**)	284.8	161.9	234973	25734
d-C16 (**5**)	284.8	161.8	246991	23946
m-C16 (**2**)	284.8	161.9	282767	20110

[a] We report average values of four independent measurements. BEs were referenced to $Au_{(4f7/2)}$ at 84.0 eV. Measured values of $Au_{(4f)}$ integrated peak areas were always within ±1% of those reported. Measured values of C_{1s} integrated peak areas were always within ±2% of those reported.

multilayer films and (2) the orientation/packing of the chains is different than those generated from 2,2-dialkylpropane-1,3-dithiols and from normal alkanethiols. We interpret the lower thicknesses of the 2-monoalkylpropane-1,3-dithiol SAMs to reflect the low density of the alkyl chains, which can lead to an increased chain tilt and/or void space in these films. Since, however, optical anisotropy can have a significant effect on the ellipsometric comparisons of films having different structures,[27] the final interpretation should be regarded with some degree of reservation in the absence of other supporting data.

XPS has been used to evaluate the nature of the chemical bond between an adsorbed alkanethiol and a metal.[28,29] In addition, XPS can provide the relative atomic composition present on the surface.[30] A comparison of the relative amounts of C, S, and Au should, in the present system, provide information regarding the packing densities in these new films. We examined three samples by XPS—**m-C16** (**2**), **d-C16** (**5**), and **n-C16** (**8**)—each characteristic of the three types of SAMs under consideration here. The results from these studies are shown in Table 2 and Figure 2. For normal alkanethiols, the formation of a gold–thiolate bond shows a binding energy (BE) for $S_{(2p3/2)}$ at ca. 162 eV.[28,29] Since all three classes of SAMs examined here exhibit $S_{(2p3/2)}$ binding energies within 0.2 eV of this value, we conclude that all S atoms are bonded to the surface of gold. Unbound thiols, which exhibit BEs for $S_{(2p3/2)}$ at ca. 164 eV and might indicate incomplete adsorbate attachment and/or multilayer formation,[29] were not detected. In addition, the absence of oxygen-bound sulfur peaks at ca. >166 eV suggests that no oxidation of these SAMs occurred during monolayer formation or characterization.[31]

Quantitative analysis of the atomic composition of SAMs by XPS requires careful consideration of the manner in which the detected photoelectrons are attenuated by any overlying material.[32] Table 2 shows the integrated peak areas of the $Au_{(4f)}$ and $C_{(1s)}$ regions obtained for all three "C-16" films using an identical protocol for each type of film. Since the observed intensities of Au and C depend on the amount of adsorbed carbon overlayer, the density of the alkyl chains in the chelating dithiol SAMs relative to that in normal alkanethiol SAMs can be determined by comparing the data collected for the chelating dithiol films with standard intensities determined for normal alkanethiol films having known overlayer thicknesses and packing densities. To this end, we constructed reference curves for both the $Au_{(4f)}$ and $C_{(1s)}$ photoelectron intensities

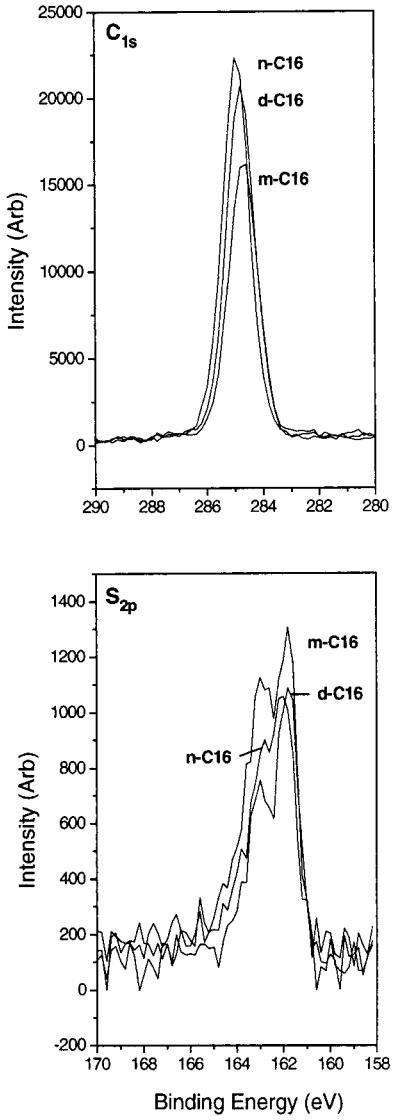

Figure 2. XPS spectra of the $C_{(1s)}$ and $S_{(2p)}$ regions for SAMs generated from hexadecanethiol (**8** ≡ **n-C16**), 2,2-ditetradecylpropane-1,3-dithiol (**5** ≡ **d-C16**), and 2-tetradecylpropane-1,3-dithiol (**2** ≡ **m-C16**).

from a series of SAMs generated from normal alkanethiols of increasing chain length (i.e., C_{12}, C_{14}, C_{16}, C_{18}, and C_{20}). For the $Au_{(4f)}$ signals measured on each SAM, we plotted the natural logarithm of the observed intensity versus the number of carbon atoms per adsorbate that attenuate the gold photoelectrons. In this analysis, we assumed that attenuation by each sulfur atom was equivalent to attenuation by 1.5 carbon atoms[33] and then normalized the data accordingly. For the $C_{(1s)}$ signals measured on each SAM, we plotted the absolute observed intensity versus the actual (i.e., unnormalized) number of carbon atoms per adsorbate.[34] We treated the molecules in the normal alkanethiol SAMs as rigid rods with a length of 1.27 Å per methylene unit, tilted 30° from the surface normal.[3] A least-squares analysis of the $Au_{(4f)}$ data then yielded an attenuation length of 42 Å, in agreement with the value quoted by Bain et al.[32]

From the curves in the plots, we determined an effective number of carbon atoms per adsorbate for both types of

(27) Gupta, V. K.; Abbott, N. L. *Langmuir* **1996**, *12*, 2587.
(28) Laibinis, P. E.; Whitesides, G. M.; Allara, D. L.; Tao, Y.-T.; Parikh, A. N.; Nuzzo, R. G. *J. Am. Chem. Soc.* **1991**, *113*, 7152.
(29) Castner, D. G.; Hinds, K.; Grainger, D. W. *Langmuir* **1996**, *12*, 5083.
(30) Hutt, D. A.; Leggett, G. J. *J. Chem. Phys.* **1996**, *100*, 6657.
(31) Schoenfisch, M. H.; Pemberton, J. E. *J. Am. Chem. Soc.* **1998**, *120*, 4502.
(32) Bain, C. D.; Whitesides, G. M. *J. Phys. Chem.* **1989**, *93*, 1670.
(33) Harder, P.; Grunze, M.; Dahint, D.; Whitesides, G. M.; Laibinis, P. E. *J. Phys. Chem. B* **1998**, *102*, 426.
(34) No correction for the presence of sulfur was needed here since sulfur does not contribute to the attenuation of the carbon signal.

Table 3. Contact Angles of SAMs and Polyethylene Films

angle	**1**−**3**[b]	**4**−**6**[b]	**7**−**9**[b]	PE branched	PE linear
$\theta_a^{H_2O}$	109	114	114	102	103
θ_a^{HD}	34	48	49	<10	<10

[a] Values of $\theta_a^{H_2O}$ were reproducible within ±2° of those reported; values of θ_a^{HD} for compounds **1**−**3** and normal alkanethiols varied more widely (±3°). [b] We report average values for inclusive chain lengths (C14, C16, and C17).

chelating dithiol SAMs. We then converted the effective number of carbon atoms per adsorbate into a relative density of adsorbates and ultimately into an relative density of chains by considering the stoichiometry of each type of adsorbate.[35] This analysis yielded from the Au intensities the following values of chain density (relative to 100% packing density for **n-C16**): **m-C16** = 61 ± 1% and **d-C16** = 94 ± 2%; and similarly from the C intensities: **m-C16** = 63 ± 2% and **d-C16** = 92 ± 3%.[36]

Contact angle measurements provide a highly sensitive tool for analyzing the composition and structure of interfaces.[1] Hexadecane, for example, can be used to detect small differences in the nature of nonpolar species that comprise an interface (e.g., methylene vs methyl groups).[9,37] Water, on the other hand, is less sensitive to this type of difference;[9,10] it is, however, highly sensitive to the presence of small quantities of polar interfacial species.[9] We used these two test liquids to characterize the SAMs generated from the 2-monoalkylpropane-1,3-dithiols. The data in Table 3 show that both liquids wet the new SAMs more than they wet the densely packed SAMs. Hexadecane, in particular, shows an enhanced wettability: $\Delta\theta^{HD} \sim 15°$. Since hexadecane is known to wet interfacial methylene groups more than it wets interfacial methyl groups,[38,39] we infer from the data in Table 3 that SAMs of the 2-monoalkylpropane-1,3-dithiols are poorly ordered and/or highly tilted, exposing a substantial fraction of methylene groups at the interface. Similarly, the wettability by water is also enhanced on the monoalkanedithiol SAMs, but the effect is less pronounced ($\Delta\theta^{H_2O} \sim 5°$). This trend is also consistent with the known enhanced wettability of water toward methylene groups vs methyl groups.[6,40]

We also compared the contact angles of hexadecane and water on the 2-monoalkylpropane-1,3-dithiol SAMs to those obtained on films of branched and linear polyethylene (PE) deposited on glass. The data in Table 3 show that both liquids wet the PE films more than they wet the monoalkanedithiol SAMs. Since the PE films undoubtedly possess a greater ratio of CH_2/CH_3 groups than do the SAMs, the data in Table 3, when taken as a whole, indicate that the interfacial structure/composition of the monoalkanedithiol SAMs falls between that of the densely packed SAMs and the PE films. Consequently, it appears that both the methylene backbones and the methyl tailgroups of these new SAMs exert substantial influence upon the interfacial wettability. Furthermore, given the observed relative values of the contact angles of hexadecane: θ_a^{HD} = 48° (dialkyl), 34° (monoalkyl), and ~10° (PE), one might be tempted to infer that the interfaces of the monoalkanedithiol SAMs consist predominantly of methyl rather than methylene moieties. Differences, however, in the packing densities of the films and/or interfacial solubilities of hexadecane might also rationalize the observed contact angle values.[6]

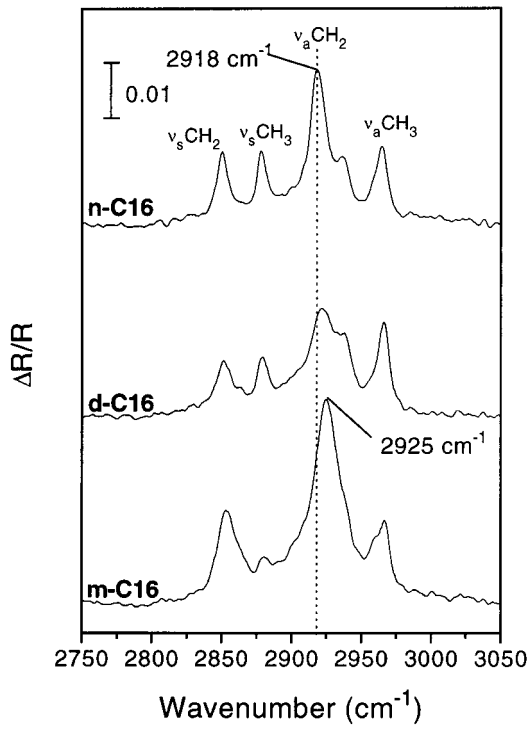

Figure 3. PM-IRRAS spectra of SAMs generated from hexadecanethiol (**8** ≡ **n-C16**, top), 2,2-ditetradecylpropane-1,3-dithiol (**5** ≡ **d-C16**, center), and 2-tetradecylpropane-1,3-dithiol (**2** ≡ **m-C16**, bottom). The differential surface reflectivity ($\Delta R/R$) was calculated as the ratio $(R_p - R_s)/(R_p + R_s)$, where R_p and R_s represent the reflectivity for the respective polarizations of light.

Surface infrared spectroscopy, such as PM-IRRAS,[41] can be used to evaluate the structural and conformational features of organic thin films.[42] In particular, both the frequency and the bandwidth of the methylene asymmetric C−H stretch (d^-) are highly sensitive to the conformational order of the films.[43,44] Figure 3 shows the PM-IRRAS spectra for representative SAMs derived from the chelating alkanedithiols **d-C16** (**5**) and **m-C16** (**2**) and a normal alkanethiol **n-C16** (**8**) having the same chain length. The d^- stretch of the monoalkanedithiol SAM appears at 2925 cm^{-1}, which is shifted to a substantially higher wavenumber than those of the SAMs derived from the spiroalkanedithiol (2921 cm^{-1}) and the normal alkanethiol (2918 cm^{-1}). This shift provides strong support that the conformational order of the SAMs decreases in the following order: *n*-alkanethiol > spiroalkanedithiol > monoalkanedithiol.[43,44] In the spectrum of the monoalkanedithiol SAM, the broad width and strong intensity of this band

(35) The stoichiometric number of carbon atoms per adsorbate is **m-C16** = 17, **d-C16** = 31, and **n-C16** = 16. Due to presence of sulfur, the stoichiometric number of carbon atoms per adsorbate used in the Au calculations is thus **m-C16** = 20, **d-C16** = 34, and **n-C16** = 17.5.

(36) Errors in the reported chain densities were determined by propagating the errors associated with the observed $C_{(1s)}$ and $Au_{(4f)}$ intensities (2% for $C_{(1s)}$ and 1% for $Au_{(4f)}$, respectively, which were determined from the average standard deviation of four measurements) throughout the calculations.

(37) Gupta, V. K.; Miller, W. J.; Pike, C. L.; Abbott, N. L. *Chem. Mater.* **1996**, *8*, 1366.

(38) Tao, Y.-T. *J. Am. Chem. Soc.* **1993**, *115*, 4350.

(39) Tao, Y.-T.; Lee, M.-T.; Chang, S.-C. *J. Am. Chem. Soc.* **1993**, *115*, 9547.

(40) Holmes-Farley, S. R.; Reamey, R. H.; McCarthy, T. J.; Deutch, J.; Whitesides, G. M. *Langmuir* **1985**, *1*, 725.

(41) Anderson, M. R.; Evaniak, M. N.; Zhang, M. *Langmuir* **1996**, *12*, 2327.

(42) Allara, D. L. In *Characterization of Organic Thin Films*; Ulman, A., Ed.; Butterworth-Heinemann: Boston, 1995; pp 57−86.

(43) Nuzzo, R. G.; Dubois, L. H.; Allara, D. L. *J. Am. Chem. Soc.* **1990**, *112*, 558.

(44) Nuzzo, R. G.; Fusco, F. A.; Allara, D. L. *J. Am. Chem. Soc.* **1987**, *109*, 2358.

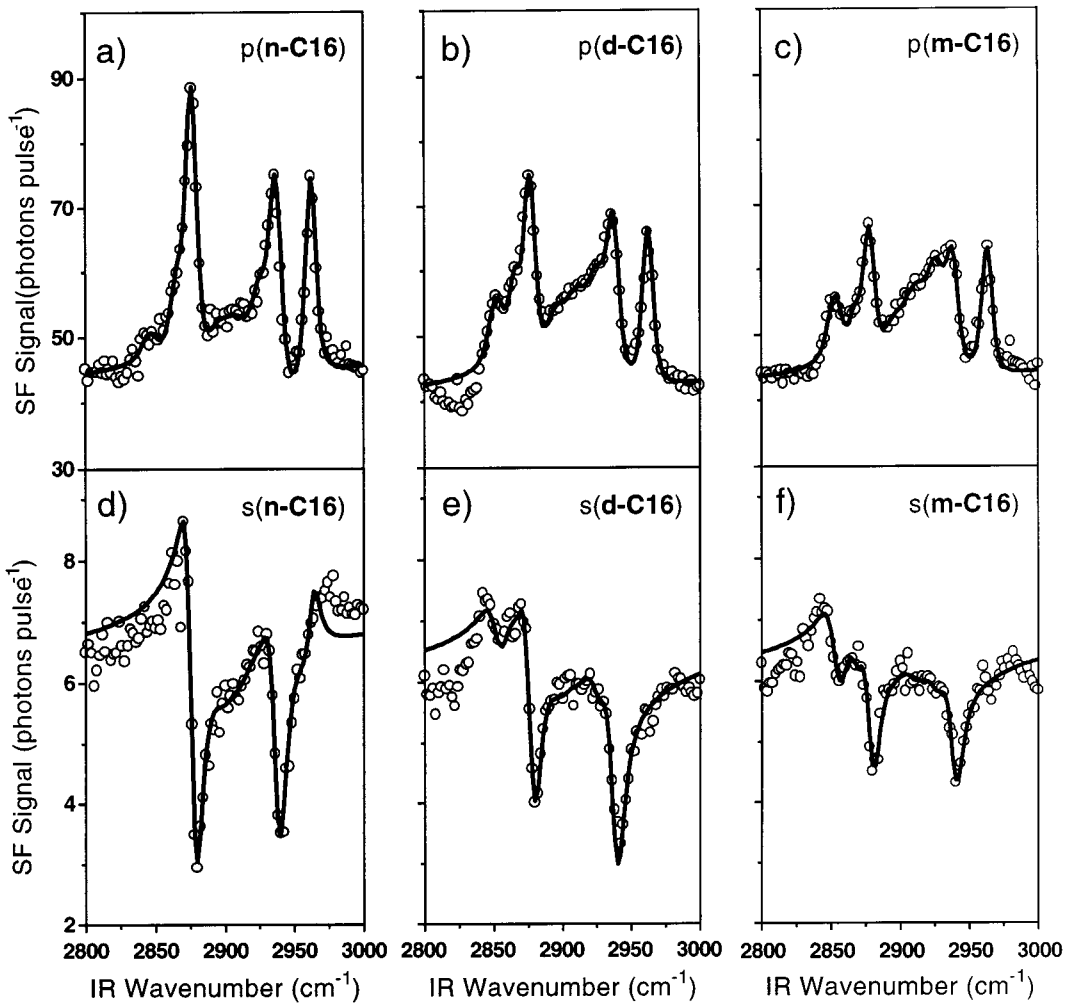

Figure 4. Sum-frequency generation (SFG) spectra of SAMs generated from hexadecanethiol (**8** ≡ **n-C16**; a and d), 2,2-ditetradecylpropane-1,3-dithiol (**5** ≡ **d-C16**; b and e), and 2-tetradecylpropane-1,3-dithiol (**2** ≡ **m-C16**; c and f). The circles represent the actual data, and the lines correspond to calculated fits to the data as described in the Experimental Section.

Table 4. Line Strengths, *S*, in SF Spectra (Arbitrary Units)

compound	S_{r^+} (ssp)	S_{d^+} (ssp)	S_{r^+} (ppp)	S_{d^+} (ppp)	S_{r^+}/S_{d^+} (ssp)	S_{r^+}/S_{d^+} (ppp)
n-C16 (**8**)	1.69		1.52	0.19	>15	8.0
d-C16 (**5**)	1.13	0.32	1.19	0.51	3.5	2.3
m-C16 (**2**)	0.71	0.47	0.83	0.51	1.5	1.6

provide further support that the alkyl chains in these types of SAMs are less crystalline and perhaps more tilted than those of densely packed films.[45]

The sum-frequency spectra of SAMs on gold derived from **n-C16** (**8**), **d-C16** (**5**), and **m-C16** (**2**) are shown in Figure 4, together with theoretical fits to the spectra. Table 4 displays the line strengths of selected modes. Of the eight independent polarization combinations, only two give significant sum-frequency signals: ppp and ssp. The SF signal obtained with s-polarized IR is too weak to observe due to the high degree of cancellation of the electric fields in the incident and reflected beams, while the spp and psp combinations are zero by symmetry.[46] The ppp spectrum is an order of magnitude stronger than the ssp spectrum but is difficult to interpret quantitatively due to contributions from both the xxz and zzz components of the nonlinear susceptibility of the monolayer, $\chi^{(2)}_R$. The ssp spectrum, though much weaker, derives solely from the yyz component of $\chi^{(2)}_R$. For this polarization, the line strength of the r^+ mode is, to a good approximation, proportional to $N\langle\cos\theta\rangle$, where N is the number of chains per unit area of the surface and θ is the angle between the C_3 axis of the methyl group and the surface normal.[47] (Note that θ is not the same as the chain tilt.) To deduce information about θ, we first need to know N. While, in principle, the relative values of N can be obtained from SF spectra,[48] it is more reliable in practice to use the chain densities derived from an analysis of the XPS data. Relative to a value of 1 for the **n-C16** SAM, the chain densities are 0.62 and 0.93 for the **m-C16** and **d-C16** SAMs, respectively. From the measured line strengths of the r^+ mode in the ssp spectrum, we find that the values of $\langle\cos\theta\rangle$ for the **m-C16** and **d-C16** SAMs are 0.68 and 0.72, respectively, relative to the value of $\langle\cos\theta\rangle$ in a monolayer of **n-C16**. For monolayers lacking any crystalline order, a decrease in $\langle\cos\theta\rangle$ indicates an increase in the average chain tilt, α, since $\langle\cos\theta\rangle \propto \langle\cos\alpha\rangle$, after averaging over all chain twists.[49] For crystalline mono-

(45) Allara, D. L.; Nuzzo, R. G. *Langmuir* **1985**, *1*, 52.
(46) Shen, Y. R. *Principles of Nonlinear Optics*; Wiley: New York, 1984.
(47) Bell, G. R.; Bain, C. D.; Ward, R. N. *J. Chem. Soc., Faraday Trans.* **1996**, *92*, 515.
(48) Bain, C. D. In *Modern Methods of Characterization of Surfactant Systems*; Binks, B. P., Ed.; Marcel Dekker: New York, 1999.
(49) Braun, R.; Casson, B. D.; Bain, C. D. *Chem. Phys. Lett.* **1995**, *245*, 326.

layers, the value of $\langle\cos\theta\rangle$ depends also on the direction of the chain tilt: for example, the line strength of the r^+ mode in monolayers of normal alkanethiols on gold shows an odd−even intensity variation despite the invariance of the chain tilt.

SF spectra also provide structural information regarding the presence of gauche defects in hydrocarbon chains. The selection rule for sum-frequency generation requires vibrational modes to be both IR and Raman active. In an all-trans hydrocarbon chain, there is a local inversion center at the middle of each C−C bond. Consequently, the methylene modes break up into a set of IR-active modes and a set of Raman-active modes: neither the d^+ nor d^- modes are observed in crystalline monolayers.[50] Gauche defects in this chain can remove this symmetry element of the chain and therefore give rise to SF-active methylene vibrations. Table 4 shows the line strength of the d^+ mode together with the ratio of the line strengths of the r^+ and d^+ modes. This ratio is useful because the dependence of the line strengths on N cancels out. For the **n-C16** (**8**) SAM, the d^+ mode is very weak, as would be expected for densely packed chains with only a scattering of gauche defects. The SF spectra of both the **m-C16** (**2**) and **d-C16** (**5**) SAMs contain prominent d^+ peaks, with comparable intensities in the two spectra. On a chain for chain basis, however, the d^+ mode is stronger in the **m-C16** SAM due to the lower value of N. In most cases, the line strength of the d^+ mode and the ratio S_{r+}/S_{d+} correlates with conformational disorder in hydrocarbon chains.[25,47,51] In the **d-C16** SAM, an alternative origin for the d^+ intensity is also possible. For the two chains to lie parallel to each other, a series of gauche defects are required near the quaternary carbon atom linking the chains. In crystals of dialkyldimethylammonium salts, for example, a ggtgg sequence has been observed.[52]

We note one final feature of the SF spectra: the vibrational frequencies of the methyl modes decrease in the order **m-C16** > **d-C16** > **n-C16**. Studies have shown that the frequencies of these vibrations are sensitive to the polarizability of the surrounding medium and that denser packing leads to lower frequencies.[53] These data can thus be interpreted to indicate that the density of packing decreases in the order **n-C16** > **d-C16** > **m-C16**.

Discussion

Overall, the results presented here demonstrate that SAMs generated from normal alkanethiols are more conformationally ordered and more densely packed than SAMs generated from both types of chelating dithiols. Moreover, the analytical data reported here for the normal alkanethiol SAMs agree well with those reported in previous studies. Comparison of the normal SAMs to those generated from the chelating alkanedithiols thus provides a useful frame of reference in which to evaluate the structures of the latter films.

We note that the spiroalkanedithiols (**4**−**6**) generate SAMs that are comparable to those generated from normal alkanethiols, although the new SAMs are slightly less ordered as indicated by the higher frequency of the d^- bands in the IR spectra. The XPS data show that the chain densities are only slightly lower (ca. 93%) than those of normal alkanethiol SAMs (100%), which is in good agreement with the results from the ellipsometric measurements. From the collection of data presented here, we cannot offer a precise structural model for the SAMs derived from the spiroalkanedithiols. Since the XPS data indicate that the packing density of these SAMs is similar to that of the normal alkanethiol SAMs, packing constraints prohibit any significant increase in tilt. In fact, the integrated absorbance of the methylene modes in the SFG spectra of the **d-C16** (**5**) SAM appears little different from that of the SAM derived from **n-C16** (**8**), suggesting that their average tilts are similar. A number of pieces of evidence, however, suggest that their structures are different. First, the relative intensities of the r^+ and r^- modes in the IR spectra are quite different in the **n-C16** and the **d-C16** SAMs; correspondingly, the odd−even effects typically observed for normal alkanethiol SAMs are not observed for the spiroalkanedithiol SAMs.[21] Second, the value of $\langle\cos\theta\rangle$ is much smaller in the **d-C16** SAM than in the **n-C16** SAM, despite a similar value of α. Third, there appear to be a number of gauche defects in the spiroalkanedithiol SAMs, yet these cannot be associated with random chain disorder, since a liquid-like density in the chains is inconsistent with the IR spectra and contact angle measurements.

It is possible that the gauche defects detected by SFG and PM-IRRAS exist near the headgroup, thereby strongly influencing the conformational order and packing density of the spiroalkanedithiol SAMs. As in a related system in which the two alkyl chains of a quaternary dialkyldimethylammonium crystals prefer to lie parallel to each other,[52] the type of geometry near the quaternary carbon atom in **4**−**6** might induce a series of gauche defects in order for the chains to ultimately achieve a closest packed configuration. It is also possible that the two terminal methyl groups of a single adsorbed spiroalkanedithiol moiety are not coplanar, although we see no trend in the wettability data that would support this hypothesis. In addition, if the cross-sectional area per chain is higher in the spiroalkanedithiol SAMs than in the orthorhombic perpendicular structure characteristic of normal alkanethiol SAMs, one might be able to rationalize the observed increase in the d^- band frequency.

The alkyl chains of the SAMs generated from the monoalkanedithiols (**1**−**3**) are less ordered and less densely packed than those of the other two types of SAMs. The XPS data show a chain density equal to less than two-thirds of that of the normal alkanethiol SAMs, consistent with the measured ellipsometric thicknesses. The XPS data also show that all the SH groups in SAMs of the monoalkanedithiols exist in the form of thiolates and therefore are presumably bound to the surface. The surface density of thiolates in the monoalkanedithiol SAM is higher than that in normal alkanethiol SAMs (by about 20%) but not sufficiently high to lead to close packing of the hydrocarbon chains: the large amount of free volume in the chain region results in a liquid-like monolayer. The contact angles of hexadecane, vibrational frequencies of the d^-(IR) and r^+(SFG) modes, and the strength of the d^+ mode in the SF spectra all point to a conformationally disordered, liquid-like film. Relative to normal alkanethiol SAMs on gold, the increase in the intensities of the methylene modes in the IR spectra (despite the low density of chains) and the decrease in $\langle\cos\theta\rangle$ in the SF spectra correspond to an increase in the average tilt angle for the alkyl chains in monoalkanedithiol SAMs. If the density of the **m-C16** SAM were that of a liquid hydrocarbon, the

(50) The methylene group adjacent to the terminal methyl group is still observed in crystalline monolayers,[26] probably due to coupling with the strongly SF-active r^+ mode.

(51) Cuyot-Sionnest, P.; Hunt, J. H.; Shen, Y. R. *Phys. Rev. Lett.* **1987**, *59*, 1597.

(52) Okuyama, K.; Iijima, N.; Hirabayashi, K.; Kunitake, T.; Kusunoki, M. *Bull. Chem. Soc. Jpn.* **1988**, *61*, 2337.

(53) Ong, T. H.; Davies, P. B.; Bain, C. D. *Langmuir* **1993**, *9*, 7141.

average chain tilt would be 47° compared to 30° in the crystalline monolayer of the normal alkanethiol.

Conclusions

A series of new chelating 2-monoalkylpropane-1,3-dithiols (monoalkanedithiols) were synthesized and used to generate SAMs on gold that were characterized by optical ellipsometry, X-ray photoelectron spectroscopy, contact angle goniometry, IR spectroscopy, and sum-frequency generation. The results support a model in which the monoalkanedithiols generate uniform monolayer films with low densities of alkyl chains that are more conformationally disordered and more tilted than those in analogous monolayer films generated from spiroalkanedithiols or normal alkanethiols.

Acknowledgment. The National Science Foundation (CAREER Award to T.R.L.; CHE-9625003) and the Robert A. Welch Foundation (Grant No. E-1320) provided generous support for this research. R.C. gratefully acknowledges the UH Center for Mexican−American Studies and The NRC-Ford Foundation for predoctoral fellowships. We kindly thank Professor Paul E. Laibinis (MIT) for helpful advice regarding the XPS analyses.

LA981698L